Redistribution of impurities in crystallizing polymers*

P. D. Calvert and T. G. Ryan
School of Molecular Sciences, University of Sussex, Brighton BN1 9QJ, UK
(Received 5 September 1977; revised 5 January 1978)

Distributions of antioxidants and u.v. absorbers in partly and fully crystallized spherulitic polypropylene were observed by u.v. and fluorescent microscopy and by scanning electron microscopy. These additives are partly pushed ahead of the growing spherulites, and the observed distribution in quenched samples has been fitted using a computer model based on exclusion of the additives from the crystallites. Diffusion coefficients for antioxidants in polypropylene melt have been obtained in this way. In fully crystallized samples there is seen to be an impurity-rich region at the spherulite boundary and a depleted zone at the centre. This is not simply due to additive rejection but also reflects a crystallinity variation within the spherulite probably due to non-crystallizable polymeric impurities.

INTRODUCTION

During crystallization of an impure molten material, partition of solutes between the solid and liquid phases will give rise to inhomogeneous distributions of impurity. The best known example of this process is zone refining, where impurities can be swept to one end of a bar by directional solidification. The important parameters in this process are the partition coefficient (K), which is the ratio of impurity concentration in the solid to that in the liquid at the interface between the two phases; the impurity diffusion coefficients in the solid (D_S) and liquid (D_L); the rate of interface advance (G) and the degree of mixing[1].

One would expect an analogous rejection process to occur in polymers which crystallize as spherulites and Price[2] has demonstrated that a wave of non-crystallizable material is pushed ahead of a growing spherulite. Moyer and Ochs[3] have shown that a wide range of impurities are concentrated at the spherulite boundaries after crystallization.

Spherulites are not single crystals but are semicrystalline aggregates which can be thought of as consisting of lamellar crystals embedded in an amorphous matrix. The fundamental rejection process will involve partition of the impurities between the lamellae and the surrounding amorphous material. This will lead to inhomogeneities on the scale of the lamellar thickness, about 10 nm, which is too fine to be resolved optically. Keith and Padden[4] have shown that impurities are concentrated in the interlamellar amorphous regions and have described how they affect the growth rate and morphology.

This local high impurity concentration in the interlamellar regions at the growing edge of the spherulite will lead also to diffusion of the impurity away from the spherulite into the surrounding liquid. Thus a growing spherulite pushes ahead of itself a wave of impurity which can be observed optically when it is on a scale comparable to the spherulite radius. A rough analogy of this could be the wave produced by a comb moved through water. In this work we have observed this rejection of impurities by the whole spherulite and fitted the results to a model for the growth of a spherical crystal where the fine structure of the spherulite is averaged out.

In the context of polymers the term impurities covers a multitude of species which are incorporated into the crystal phase to a lesser extent than the bulk of the polymer chains. For the purposes of the model we will assume that the impurities are completely dissolved and unclustered in the molten polymer, and are not incorporated in the crystal phase to any significant extent, but remain dissolved in the interlamellar amorphous regions. These assumptions will be reasonable for many antioxidants, u.v. stabilizers and other additives, as well as atactic polymer. Low molecular weight polymer will also be rejected as the extent to which chains are incorporated into the crystal structure is a function of molecular weight, but in this case allowance would have to be made for partial crystallization. Since additives are usually present in small amounts they are unlikely to affect the spherulite morphology but segregation of large quantities of low molecular weight polymer will affect the spherulite[4]. Similar arguments could be applied to partly oxidized polymer or molecules containing other irregularities. Particulate additives and dissolved gases will also undergo segregation during crystallization of the polymer and their behaviour will be discussed in a separate paper.

EXPERIMENTAL OBSERVATIONS

In principle, additive distributions may be observed by any microscopic technique for which an additive can be found which strongly contrasts with the polymer. Moyer and Ochs[3] used autoradiography of radiolabelled additives, Frank and Lehner[5] and Curson[6] used ultra-violet microscopy of strongly absorbing compounds to observe distributions in fully crystallized polypropylene and Klein and Briscoe[7] have followed diffusion of stearates by infra-red microdensitometry.

Ultra-violet microscopy is an effective technique because a range of u.v. screening additives with very high ($10^4\,cm^{-1}\,mol^{-1}$) absorption coefficients are available and because commercial phenolic antioxidants absorb in the

* Presented at the Polymer Physics Group (Institute of Physics) Biennial Conference, Shrivenham, September 1977)

0032–3861/78/1906–0611$02.00

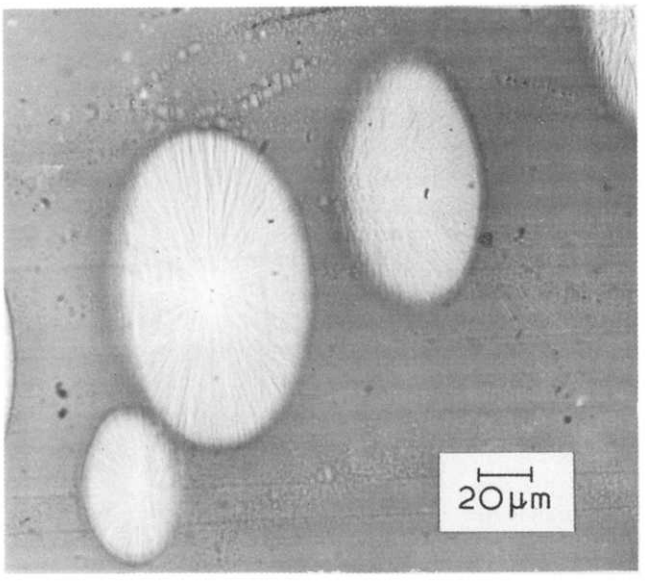

Figure 1 Polypropylene section containing 0.5% of Uvitex OB partly crystallized at 125°C and quenched. Viewed in u.v. transmission.

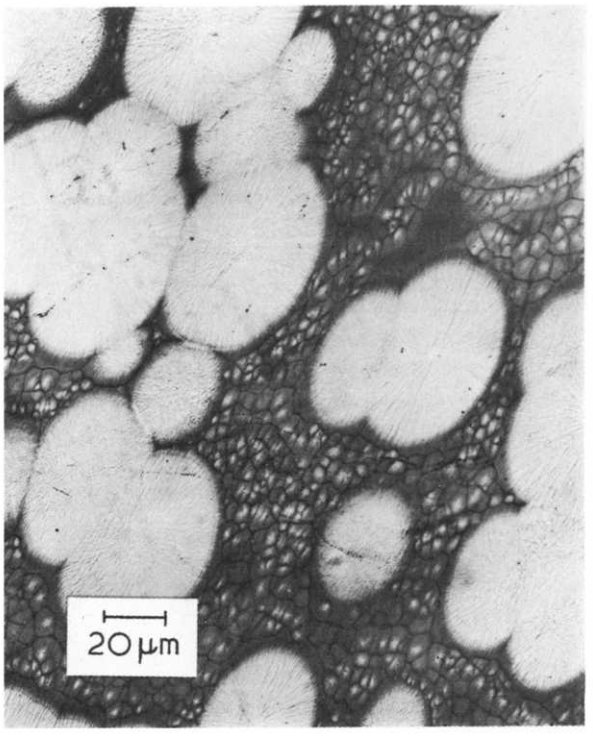

Figure 2 Polypropylene containing 1% Uvitex OB partly crystallized at 130°C and quenched. Viewed in transmission using a 325 nm laser source

ultra-violet and can be studied. The polymer used was polypropylene provided by ICI Ltd, Plastics Division, designated Type HF20, which has a single peak molecular weight distribution with $\bar{M}_w$ and $\bar{M}_n$ in the regions of 580 000 and 70 000, respectively. The atactic content was estimated to be 5%. Additives were incorporated by mixing the polymer with a solution of the additive in dichloromethane. Irganox 1010 (0.1%) was added as an antioxidant. Samples were moulded at 220°C then melted at 240°C for about 2 min and crystallized isothermally. At the concentrations used, the additives do not noticeably change the crystallization rate of the polymer. *Figure 1* shows a 10 μm section of a sample containing Uvitex OB [2,5-di(5-t-butyl-2-benzoxazolyl)thiophene] (0.5%) an optical brightener. This sample was partly crystallized at 125°C and quenched to freeze in the wave of material rejected ahead of the spherulites. This wave can be analysed more simply than the fully crystallized distribution. The micrograph was taken in u.v. transmission at 325 nm. The mounting medium used was glycerol which does not leach the additives out of the polymer. In these quenched samples the spherulites deform somewhat during room temperature sectioning and appear elliptical.

In *Figure 1* it can be seen that there is a reduced additive concentration within the spherulite, a local high concentration around the boundary and a dip at the spherulite centre. *Figure 2* shows a similar micrograph taken with a 325 nm He–Cd laser as a light source. We believe that the considerably better resolution results because the light is monochromatic.

Uvitex OB can also be observed in fluorescence as shown in *Figure 3*. This mode would be expected to be more sensitive at low additive concentrations and does tend to show the dip in concentration at the spherulite centre more clearly. These techniques have been extended to a number of antioxidants although they are more difficult to observe as their absorption coefficients are lower than those of the u.v. absorbers.

Quantitive distribution data were obtained by scanning the negatives of these micrographs using a double beam microdensitometer. A series of fully quenched samples containing different additive concentrations were used to provide a calibration plot between micrograph optical density and concentration. In the partly crystallized and quenched samples the quenched regions distant from the spherulites could also be used for calibration. We estimate that relative concentrations within any micrograph can be found to ±5% but between pictures errors are of the order of ±20%. The spherulites themselves are not uniform but show a fibrillar structure which appears as noise on the microdensitometer traces. The significance of this inhomogeneity will be discussed in a subsequent paper.

Distributions were also measured for a nickel-containing

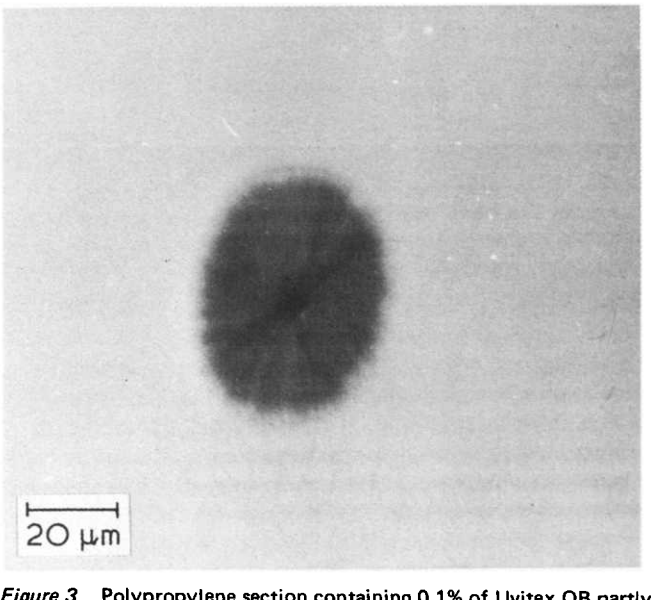

Figure 3 Polypropylene section containing 0.1% of Uvitex OB partly crystallized at 130°C and quenched. Viewed by fluorescence.

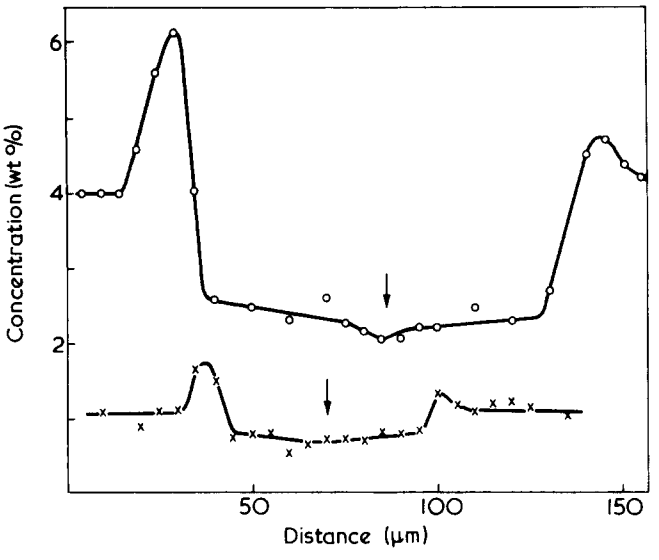

Figure 4 Nickel distribution by EDAX for UV1084 in polypropylene partly crystallized at 130°C and quenched. ○, 4 wt % UV1084; X, 1 wt % UV1084, ↓ spherulite centre

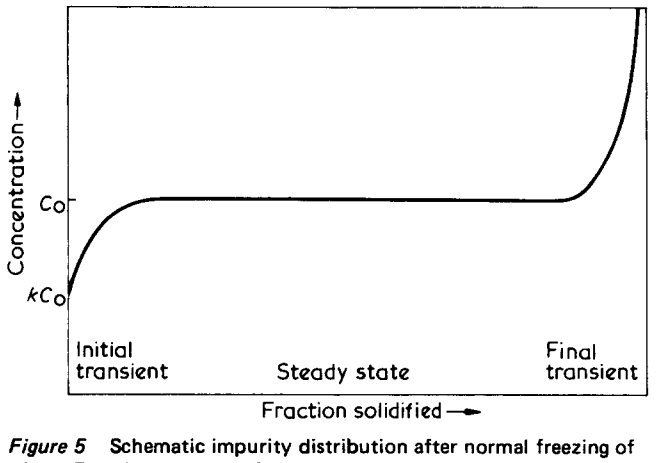

Figure 5 Schematic impurity distribution after normal freezing of a bar. Freezing starts at left. C_0 is initial concentration; K is the partition coefficient

additive using an Ortec energy dispersive X-ray analysis system (EDAX) mounted on a Cambridge Stereoscan scanning electron microscope. The distributions of UV 1084 ([2,2-thiobis(4-t-octyl phenolato)] n-butylamine nickel) in polypropylene partly crystallized at 130°C and quenched are shown in *Figure 4*. Measurements were made by point counting along spherulite radii during which time the polymer clearly degraded but without apparent loss or migration of the nickel. Microtomed sections and crystallized thin films gave similar results. Again a boundary peak and lowered concentration within the spherulite are observed and there is some sign of a central dip. However, this method did not have such good sensitivity or resolution as the u.v. methods.

Computer model

The calculation for the redistribution of a soluble impurity during crystallization is similar to that given by Pfann[1] for 'normal' freezing wherein a liqud is solidified from one end. The ratio of impurity concentration in the solid to that in the liquid at the interface is given by the partition coefficient. If diffusion in the liquid is compared to that in the solid, and there is no convective mixing, the excess impurity diffuses away into the liquid down a concentration gradient. The final distribution shows an initial transient over which the concentration increases to a steady state value and a final transient where the concentration increases as shown in *Figure 5*. The width of the initial and final transients is of the order of D_L/G where D_L is the liquid diffusion coefficient and G the growth rate.

For polymer spherulites the calculation is similar except that spherical corrections are added to the diffusion equations. In the computation a mass balance is written for the interface and diffusion equations for the solid and liquid regions. Mirror conditions are applied at the spherulite centre and the final boundary, the position the spherulite would reach when fully grown. This has the effect of mimicking a ring of spherulites growing inwards to collide with the one being observed. This is a fairly realistic situation but does not allow analysis of triple meeting points or any non-spherical symmetry. Computation is carried out at a series of time steps in which the interface is moved by one distance unit and all the concentrations recalculated for diffusion using the Crank–Nicholson method[8]. Crank[8] described the choice of appropriate time and distance steps in these calculations. The crucial part of the calculation is obtaining the correct interface equations and this can be checked by determining the change in the total amount of impurity in the system after computation. Typically the model loses 0.002% of the impurity during a run.

The partition coefficient is taken to be equal to the amorphous content of the spherulite at the interface, that is, 1 – (crystallinity). This follows from assuming that very little additive is incorporated into the crystals and that, at this point, the interlamellar amorphous regions are essentially identical to the liquid. The growth rate and spherulite radius are known and the additive diffusion coefficients are used as fitting parameters for the observed distributions.

Figure 6 shows a set of distributions calculated for a spherulite crystallized at 125° to 30% of its final radius, for a series of additive diffusion coefficients in the liquid and no solid state diffusion. *Figure 7* shows the effect of diffusion

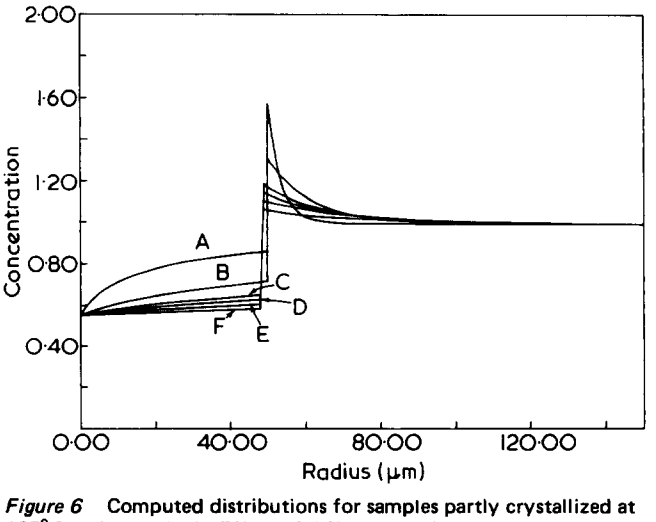

Figure 6 Computed distributions for samples partly crystallized at 125°C and quenched. Effect of diffusion coefficient in liquid, no solid state diffusion. *DL* = Diffusion coefficient of additive in liquid (μm^2/sec); *DS* = back diffusion coefficient; *G* = spherulite growth rate (μm/sec). Concentration profiles. Partition coefficient = 0.55. A, *DS* = 0.000, *DL* = 1.000, *G* = 0.250; B, *DS* = 0.000, *DL* = 5.000, *G* = 0.25; C, *DS* = 0.000, *DL* = 10.000, *G* = 0.25; D, *DS* = 0.000, *DL* = 15.000, *G* = 0.250; E, *DS* = 0.000, *DL* = 25.000, *G* = 0.250; F, *DS* = 0.000, *DL* = 50.000, *G* = 0.250

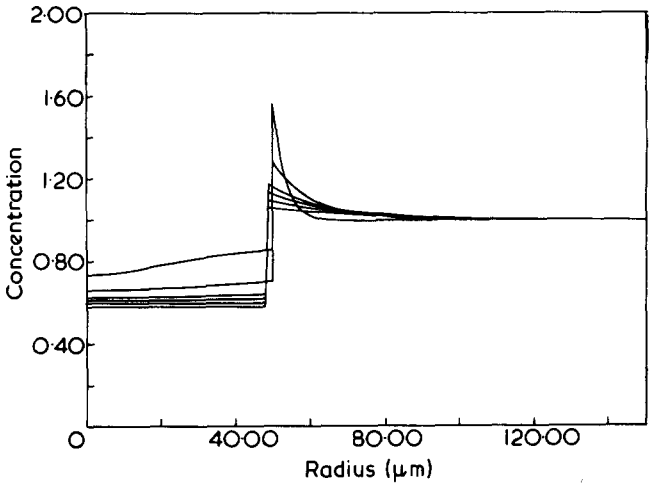

Figure 7 Computed distributions for samples partly crystallized at 125°C and quenched. Effect of diffusion coefficient in liquid, with solid state diffusion. *DL* = Diffusion coefficient of additive in liquid (μm^2/sec); *DS* = Back diffusion coefficient; *G* = spherulite growth rate (μm/sec). Partition coefficient = 0.55. A, *DS* = 0.333, *DL* = 1.000, *G* = 0.250; B, *DS* = 1.667, *DL* = 5.000, *G* = 0.250; C, *DS* = 3.333, *DL* = 10.000, *G* = 0.250; D, *DS* = 5.000, *DL* = 15.000, *G* = 0.250; E, *DS* = 8.333, *DL* = 25.000, *G* = 0.250; F, *DS* = 16.667, *DL* = 50.000, *G* = 0.250

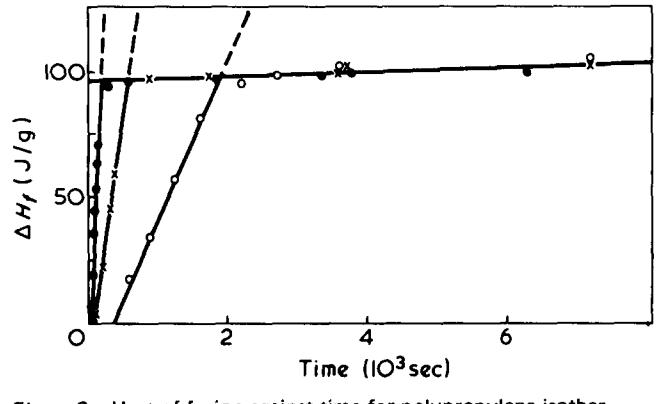

Figure 8 Heat of fusion against time for polypropylene isothermally crystallized at ●, 120°C; X, 125°C; ○, 130°C

within the spherulite (D_S). These show the same general features as *Figures* 1–4, a lowered spherulite concentration, a boundary peak and a central dip.

The crystallinity of the growing spherulite interface was estimated by crystallizing the polymer in a scanning calorimeter (Perkin–Elmer DSC-2) for varying times at 125°C, then increasing the temperature to measure the heat of fusion. The break in the plot of heat of fusion *versus* time at 10 min (*Figure 8*) was taken to correspond to the end of spherulite growth. The intercept of the secondary growth line at zero time was used to calculate a 'primary' crystallinity and hence a partition coefficient. This method is not rigorous but the curves are not very sensitive to partition coefficient in this range.

Thus we have a model which assumes dissolved impurities at low concentrations, uniform growth rates and diffusion coefficients no convection in the liquid, no interlamellar secondary crystallization, no impurity in the crystals and a spherulite structure which is homogeneous on the scale of observation. Qualitatively the distribution pattern resembles that observed.

Quantitative fit of model to results

Figure 9 shows the degree of fit between experimental and theoretical distribution curves for Uvitex OB in polypropylene partly crystallized at 125°C. Two theoretical curves for liquid diffusion coefficients of 5 and 10 μm^2/sec are shown and by fitting the shape of the interface peak in this way it is possible to obtain a value for the antioxidant diffusion coefficient in the melt. This fitting procedure is insensitive to the crystallinity and to diffusion within the spherulite, but there are a number of other effects which may introduce errors.

Edge effects can arise due to refractive index mismatches in the system. These sill give sharp bright and dark lines at the spherulite boundaries which can be distinguished from concentration effects and eliminated by careful focusing. The finite thickness of the films will broaden the observed boundary peak if the spherulite is small, so that its boundary is strongly curved. This can be accounted for by introducing a correction term into the computed distributions, but is rarely important. Overlap of the diffusion fields of neighbouring spherulites can have a marked effect on the shape of the observed distribution, and cannot be satisfactorily corrected in the calculations as the situation of two approaching spherulites lacks spherical symmetry. This can be overcome by quenching samples at low conversions and by ensuring that the distribution is symmetrical around a spherulite. Finally, in order to obtain a well resolved boundary peak it is necessary that the ratio D_L/G is in the range of 1–20 μm; otherwise the peak is either too sharp or is lost in the background. This means for polypropylene that the diffusion rate must fall in the range from 0.01–10 μm/sec if accurate measurements are to be made at some temperature where partial crystallization and quenching is possible.

From *Figure 9* it can also be seen that whilst the model can give a reasonable fit to the boundary peak no central dip is predicted. Comparison of *Figure 9* with *Figure 6* shows that for a central dip to be observed the impurity diffusion coefficient should be of the order of 1 μm^2/sec and *Figure 7* demonstrates that addition of solid state diffusion will tend to level out even this. We believe that crystallinity variations within the spherulites account for this central dip and for much of the additive distribution that is observed within fully crystallized samples. The observed distribution within spherulites is thus not only due to varying local concentrations of additive within the amorphous regions, but is pre-

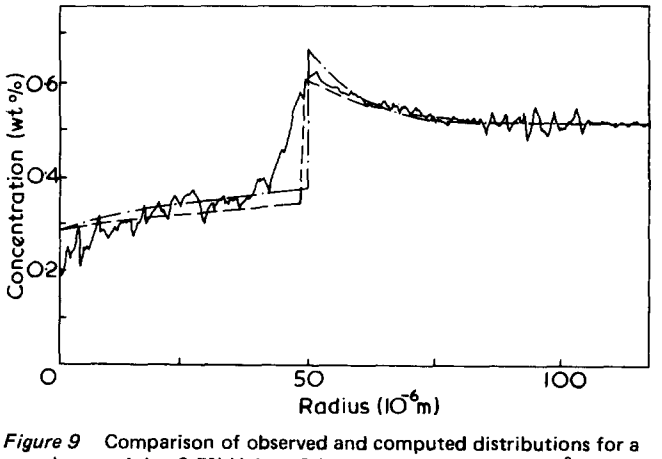

Figure 9 Comparison of observed and computed distributions for a sample containing 0.5% Uvitex OB partly crystallized at 125°C. — · —, *DL* = 5 μm^2/sec; — — —, *DL* = 10 μm^2/sec

dominantly due to varying amounts of amorphous material within the spherulite. This can be established by allowing additive to diffuse into samples which have been crystallized without additive. In this case any observed distribution will be due to crystallinity variations. *Figure 10* shows distributions in annealed samples and in a sample where additive has been diffused in from glycerol solution at 130°C. The similarity of the distributions implies that all these are due to crystallinity variations.

Keith and Padden[4,16] have applied concepts of morphological stability to polymers and conclude that high molecular weight impurities should give rise to structural effects on a scale given by D_L/G. This corresponds to the size of the fibrillar structure seen in many spherulites. They have also seen hedrite to spherulite growth forms apparently induced by the types of impurity rejection and concentration processes discussed here. A full explanation of why these central high crystallinity regions are seen would need to say why such large scale inhomogeneities should be observed in a structure which contains finely dispersed amorphous material.

This raises the question of whether the boundary peaks that are observed in quenched samples are not also due to the presence of a low crystallinity region at the boundary into which the additive moves after quenching. Movement of impurities in polypropylene at room temperature will depend on the diffusion coefficients. However, since this is close to the glass transition temperature of the polymer, extrapolation of high temperature diffusion measurements will not be at all reliable. We believe that the quenched distribution is a good representation of the distribution in the polymer during crystallization, as different additives give different distribution patterns and no change in the distribution is seen on storing at room temperature. However, as a precaution samples were stored at −40°C.

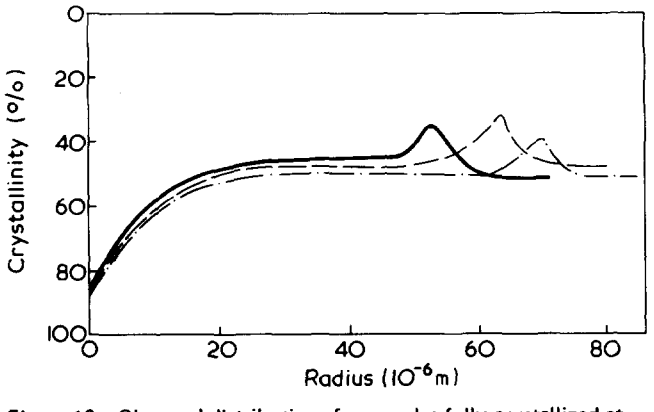

Figure 10 Observed distributions for samples fully crystallized at 130°C containing Uvitex OB. ——, Crystallized for 2 h; — — —, crystallized and annealed for 7 days; — · — · —, crystallized without additive and annealed in a solution of Ivitex OB in glycerol at 130°C

Table 1 gives measured values of the diffusion coefficient for a number of additives and antioxidants. For Ionox 330 and Uvitex OB it can be seen that as would be expected a change of growth rate of about an order of magnitude does not affect the measured diffusion coefficient, but the method is not sufficiently accurate to determine the temperature dependence of the diffusion coefficient itself. There is a general trend of decreasing diffusion coefficient with increasing molecular weight. There are no comparable measurements for the melt diffusion coefficients of these additives, but measurements have been made on similar compounds in solid polypropylene as shown in *Table 1*. From this Table it can be seen that the diffusion coefficient decreases with increasing molecular weight, and that rigid molecules diffuse more slowly than flexible molecules of the same molecular weight. All our measurements are on additives which can be classified as rigid. In the two cases where different groups have measured the same additive, their results disagree by a factor of two or three; a factor which should be borne in mind when interpreting diffusion data. Measurements on gases in rubber[11] and flexible molecules in polyethylene[7] suggest a three-fold higher diffusion rate in the melt than in the solid which is a greater difference than would be predicted on the basis of crystallinity alone. By measuring the progress of Uvitex OB diffusing into solid polypropylene at 130°C from glycerol solution, we obtain a diffusion coefficient of 10^{-8} cm^2/sec compared with 10^{-7} cm^{-2}/sec in the melt at the same temperature (*Table 1*). It seems not unreasonable to observe a ten-fold change in diffusion coefficient between melt and solid for such a large, rigid molecule.

In further publications we will discuss distributions in fully crystallized samples and the use of these techniques to measure solid state diffusion coefficients. The significance

Table 1 Observed values of additive diffusion coefficients in molten polypropylene

Additive	Molecular weight	Diffusion coefficients (cm^2 sec) 120°C	125°C	130°C
2,6-Di-t-butyl-4-methoxy phenol (Topanol 354)	236	1.0×10^{-7}	–	1.5×10^{-7}
2,2'-Methylene bis(4-methyl-6-t-butyl phenol) (CAO-5)	324	$>2.5 \times 10^{-7}$	–	$>5.0 \times 10^{-7}$
2-Hydroxy-4-octoxy benzophenone (UV531)	326	–	2.0×10^{-7}	–
2,5-Di(5-t-butyl-2-benzoxazolyl)thiophene (Uvitex OB)	430	6.0×10^{-8}	7.0×10^{-8}	$>1.0 \times 10^{-7}$
2,4,6-Tris(3,5-di-t-butyl-4-hydroxybenzyl)-1,3,5-trimethylbenzene (Ionox 330)	768	2.0×10^{-8}	2.0×10^{-8}	1.0×10^{-8}
N,N',N''-Tris(2,6-di-t-butyl-4-methyl phenyl)isocyanurate (Goodrite 3114)	777	1.0×10^{-8}	–	–
N,N',N''-Tris(ethyl[3,5-di-t-butyl-4-hydroxy phenyl]-propionate)isocyanurate (Goodrite 3125)	999	$<1.0 \times 10^{-8}$	–	–
Tetrakis(methylene 3[3',5'-di-t-butyl-4-hydroxy benzyl]-propionate)methane (Irganox 1010)	1176	$<1.0 \times 10^{-8}$	–	–

Table 2 Reported values for additive diffusion coefficients in solid polypropylene extrapolated to 120°C

Additive	Molecular weight	Measured temperature range	Diffusion coefficient (cm^2/sec)	Reference
Flexible:				
Dimethyl thiodipropionate	206	80–110	8.6×10^{-8}	12
Di-n-hexyl thiodipropionate	346	80–110	5.0×10^{-8}	12
n-Octadecyl diethanolamine	357	80–135	1.6×10^{-7}	13
Di-n-dodecyl thiodipropionate	514	80–110	3.0×10^{-8}	12
Di-n-dodecyl thiodipropionate	514	55–135	7.7×10^{-8}	13
Di-n-octadecyl thiodipropionate	682	80–110	2.0×10^{-8}	12
Rigid:				
Phenothioazine	199	80–135	2.6×10^{-7}	13
2,4-Dihydroxy benzophenone	214	50–75	4.5×10^{-7}	14
2,6-Di-t-butyl-4-methyl phenol	220	50–75	6.5×10^{-7}	13
2-Hydroxy-4-methoxy benzophenone	228	80–110	5.0×10^{-8}	12
2-Hydroxy-4-n-butoxy benzophenone	270	80–110	4.0×10^{-8}	12
2-Hydroxy-4-octoxy benzophenone	326	80–110	2.7×10^{-8}	12
2-Hydroxy-4-octoxy benzophenone	326	45–75	1.5×10^{-7}	15
2-Hydroxy-4-dodecoxy benzophenone	382	80–110	2.2×10^{-8}	12
2-Hydroxy-4-octadecoxy benzophenone	466	80–110	2.0×10^{-8}	12
1,1,3-Tris(2-methyl-4-hydroxy-5-t-butyl-phenyl)butane	544	100–150	6.5×10^{-9}	13

of these processes for the stabilization of polypropylene has been discussed elsewhere[9,10].

CONCLUSIONS

We have shown that growing polymer spherulites push a wave of rejected impurities ahead of the interface. This process can be analysed using a simple normal freezing model, treating the spherulite as a homogeneous solid. Melt diffusion coefficients have been obtained in this way for a number of u.v. absorbers and antioxidants. The impurity distributions observed by others in fully crystallized samples are not simply due to this rejection process but reflect a morphological variation within the spherulite. The high central crystallinity and low boundary crystallinity should have a marked effect on the physical properties of the polymer. The rejection model should be applicable to all spherulitic polymers providing that the appropriate growth rates and crystallinities are used. On the other hand the final distribution seems to be sensitive to secondary crystallization and may vary considerably from polymer to polymer.

ACKNOWLEDGEMENTS

Dr N. C. Billingham of the University of Sussex has been involved at all stages of this work. P. Prentice took the first u.v. micrographs and D. C. Bott has contributed to recent experiments. This project would not have been possible without the cooperation of ICI Ltd, Plastics Division, especially A. D. Curson, F. M. Willmouth and D. G. M. Wood.

We thank D. Back of Kings College, London, for the use of a u.v. microscope. T. G. R. was supported by the SRC on a Case award in conjunction with ICI Ltd.

REFERENCES

1 Pfann, W. G. 'Zone Melting' 2nd Edn, Wiley, New York, 1966
2 Barnes, W. J., Luetzel, W. G. and Price, F. P. *J. Phys. Chem.* 1961, **65**, 1742
3 Moyer, J. D. and Ochs, R. J. *Science* 1963, **142**, 1316
4 Keith, H. D. and Padden Jr, F. J. *J. Appl. Phys.* 1964, **35**, 1270
5 Frank, H. P. and Lehner, H. *J. Polym. Sci. (C)* 1970, **31**, 193
6 Curson, A. D. *Proc. R. Microsc. Soc.* 1972, **7**, 96
7 Klein, J. and Briscoe, B. J. *Polymer* 1976, **17**, 481
8 Crank, J. 'The Mathematics of Diffusion' 2nd Edn, Oxford University Press, Oxford, 1975
9 Billingham, N. C., Calvert, P. D., Prentice, P. and Ryan, T. G. 'The weathering of plastics and rubber' Plastics and Rubber Institute Symp. Proc. 1976
10 Billingham, N. C., Calvert, P. D., Prentice, P. and Ryan, T. G. *Polym. Prepr.* 1977, **18**, 476
11 Rogers, C. E. in 'Physics and Chemistry of the organic Solid State' (Eds D. Fox, M. M. Labes and A. Weissberger) Interscience, New York, 1963, Vol II
12 Dubini, M., Cicchetti, O. Vicario, G. P. and Bua, E. *Eur. Polym. J.* 1967, **3**, 473
13 Jackson, R. A., Oldland, S. R. D. and Pajaczkowski, A. *J. Appl. Polym. Sci.* 1968, **12**, 1297
14 Westlake, J. F. and Johnson, M. *J. Appl. Polym. Sci.* 1975, **19**, 319
15 Johnson, M. and Westlake, J. F. *J. Appl. Polym. Sci.* 1975, **19**, 1745
16 Keith, H. D. *J. Polym. Sci. (A)* 1964, **2**, 4339